Thermal Testing of Small Antennas in Multi-Probe Spherical Near-Field Systems

A. Giacomini, R. Morbidini, L. J. Foged

Microwave Vision Italy s.r.l.
Via dei Castelli Romani, 59
00071 Pomezia, Italy
andrea.giacomini@microwavevision.com

J. Acree, J. Estrada

MVG Inc.
2105 Barrett Park Dr, Suite 104
Kennesaw, Georgia, USA
jim.acree@mvg-us.com

E. Szpindor, P. O. Iversen

Orbit/FR Inc.
506 Prudential Road
Horsham, 19044, Philadelphia, USA
peri@orbitfr.com

Abstract— **Temperature changes cause thermal expansion of antenna materials and will have an important impact on antenna performances. In some applications, it is sufficient to calculate the antenna deformation by mechanical analysis and determine the RF impact by EM analysis tools. However, if the environmental conditions of the final antenna are stringent and considered critical as in the case of military and civil applications like space and aeronautics, the thermal performance of the antenna must be determined by experiment [1]-[2].**

Based on the preliminary results discussed in [3], this paper present a simple and effective method for thermal testing of antennas in a spherical near field range based on multi probe technology [4]–[9]. The antenna is maintained inside an RF transparent thermally insulated container including the local heating and cooling equipment. The fast testing provided by the multiprobe system allows one to measure the temperature dependence of the antenna at several different temperatures within the investigation range. The method will be illustrated for the cold measurement case with temperatures below -100°C but the extension to the full cold to hot temperature range is trivial.

I. INTRODUCTION

In many common antenna applications in the temperature ranges of typical commercial purposes, the effect of temperature on the antenna's performances can be either neglected or if necessary, determined from mechanical analysis with the RF impact established by EM analysis tools. Antennas designed for demanding environmental applications like military, space, avionic etc. have stringent constraints on the allowed dependence of the antenna performances within the operating temperature range. Often it is necessary to test the device in realistic temperature conditions to verify its compliance and correct functionality. The typical temperature testing ranges are between -50°C and +80°C but the range can also be even more extensive.

A very general approach for thermal testing of antennas at different temperatures is to enclose the antenna with a closed but RF transparent climate box and investigate the temperature dependence of the antenna by evaluating the relative changes in the antenna performance while in the climate box [1]-[2]. The main function of the climate box is to ensure that only the temperature of the antenna is varied while the measurement system and other equipment are maintained at a constant temperature. This is mandatory to preserve the measurement accuracy.

Other than being a complex measurement setup, this approach also suffers from the drawback that the climate box is in a fixed position with respect to the measurement chamber. This is to allow temperature control which is external to the climate box. The antenna however, is rotated on its positioner, often in a classical azimuth over elevation configuration. This means that the antenna "sees" a different reflective environment for each direction since the antenna is rotated with respect to the climate box and this can affect the quality of the measurement, unless the climate box is completely RF transparent.

The method presented in this paper is simple and effective. The antenna is maintained inside an RF transparent thermally insulated container including the local heating and cooling equipment. The cooling of the Antenna Under test (AUT) is provided by means of heat conduction with liquid nitrogen, which is fairly common and easy to procure. In the case of heating, simple local heating equipment is used. The climate box rotates with the antenna to provide a stable scattering environment for the antenna. Using a multiprobe system the mechanical rotation of the antenna is only in the azimuth direction. It is worth noting that the fast testing provided by the multiprobe system allows to measure the temperature dependence of the antenna at several different temperatures within the same experiment.

Examples of measurements on a helix antenna will be shown. The antenna under test is a quadrifilar helix with an isoflux pattern suitable for TT&C applications. The quadrifilar

helix is an antenna that could be potentially sensitive to temperature variation due to the use of dielectrics in the support.

The test has been carried out at low temperatures, which in practice is more important than high temperature for avionic applications. The extension to the full cold-hot temperature range is trivial.

The organization of this paper follows: Section II introduces the MVG StarLab near field measurement facility, briefly describing the system itself and its performances; Section III goes into a detailed description of the setup of the thermal measurement system that has been used in the actual experiment; Section IV shows the preliminary results obtained during a low temperature thermal cycle.

II. STARLAB MEASUREMENT FACILITY

The spherical near field antenna measurement system StarLab is based on patented probe array technology [4]–[9] and is shown in Figure 1. The probe array is composed of two sets of dual polarized probes to cover the full 0.8-18GHz band. The two arrays are interleaved and fully integrated in the structure of the system. StarLab system offers the speed advantages of a probe array while the mechanical rotation in elevation allows for unlimited angular resolution over the full 3D sphere.

Figure 1.   StarLab: 650MHz to 18GHz Spherical Near Field Antenna Measurements System.

StarLab is mainly aimed at the characterization of electrically small antennas and wireless terminals for development, pre-qualification or pass/fail production purposes. A key feature of the system is its compactness and portability allowing it to be used directly in laboratories or production centers without extra logistics. The probes are completely reciprocal and can be used both in receive and transmit modes. The probe array elements are mounted on a circular arch and embedded in multi-layer conformal absorbers. The probe tips protrude through small crossed slots in the smooth curvature of the absorbers keeping the reflectivity of the probe array at a minimum. The absorbing material also reduces scattering and reflections from the support structure and cabling. The internal diameter of the probe array in

StarLab is 90 cm measured from the tip of one probe to the tip of the probe on the opposite side.

III. THERMAL MEASUREMENT SETUP DESCRIPTION

The climate box has been specifically designed for the AUT and its overall dimensions are compatible with the compact near field measurement system. The cooling cycle carried out during the experiment is based on the use of liquid nitrogen, which is a widespread and relative easy procurement material in the scientific environment. Liquid nitrogen maintains temperatures far below the freezing point of water and makes it extremely useful in a wide range of applications. Nitrogen has a permittivity very close to one in its gaseous state, while it is about 1.45 in its liquid state [10].

The setup shown in Figure 2 consists of the following components:

- climate box (divided in three parts)
- immersion chiller (antenna add-on)
- liquid nitrogen
- RF feeding cables for cryogenic applications
- thermistors
- datalogger
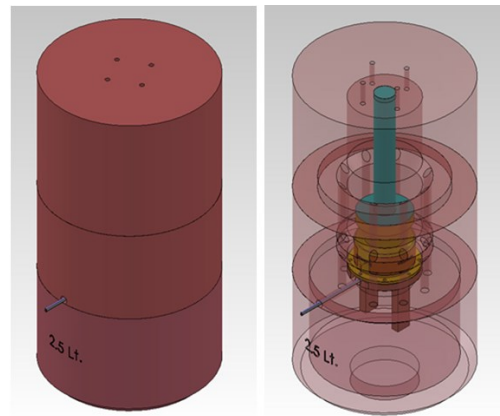
Figure 2.   Climate Box.

Externally, the climate box looks like a cylinder (ø=220mm, h=400mm) consisting of a top cover, an intermediate part and a bottom part, as shown in Figure 3. The assembly has been designed in order to ensure the maximum RF transparency.

The box is made of extruded polystyrene foam [11], which provides a good thermal insulation between the AUT, the external environment and measurement system. This is a crucial point in order to ensure that only the antenna temperature is varied while the measurement system and other equipment are maintained at a constant temperature to ensure the measurement accuracy. Each part of the climate box has been machined with high precision to accommodate the AUT and provide a perfect alignment of the antenna itself with respect to the measurement system.

The AUT cooling is achieved through heat conduction using two different techniques of heat transfer on the AUT at the same time. The container for the liquid nitrogen is the

bottom part of the climate box. An immersion chiller is fastened on the AUT and is immersed into the liquid nitrogen, ensuring the primary cooling of the AUT by conduction. Nonetheless, the airflow outlets carved in the climate box along with the four holes at its top provide a continuous dry-air flow across the whole climate box, ensuring at the same time the additional cooling of the upper part of the antenna while avoiding the build-up of condensation on the AUT.
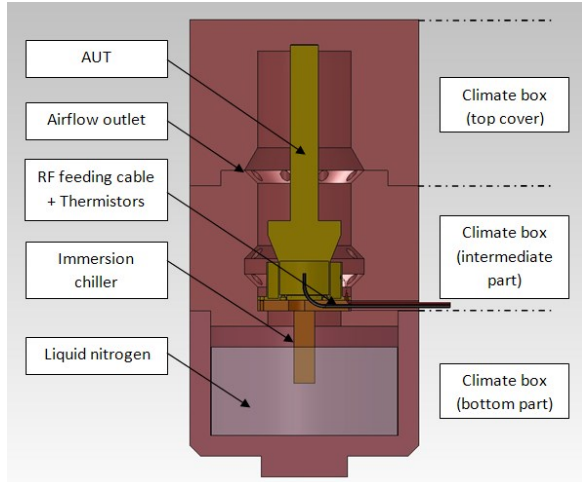
Figure 3.   Section of the climate box.

Several thermistors have been attached at different positions on the AUT and are monitored by an 8-independent-channels datalogger. Each sensor records at specific time intervals, the temperature at its given location on the surface of the AUT.

A special RF cable [12] with wide operating temperature has been utilized and the feeding point has been provided by means of a RF-cable-dedicated hole specifically carved into the climate box.

As discussed earlier, the whole thermal control design aims to be as RF transparent as possible to improve measurement accuracy. This allows a direct measurement of the radiation pattern of the cooled antenna, unlike the common approach which only evaluates the relative changes. A test has been carried out at room temperature in order to investigate the RF transparency, measuring S-parameters and pattern of the AUT in a typical free space environment, and comparing the results with the AUT enclosed inside the climate box. Figure 4 and 5 clearly show that there is no significant effect due to the presence of the climate box surrounding the antenna neither on the S parameter nor on the antenna pattern.

Figure 4 is the comparison of the return loss curve with the antenna in free space and enclosed in the climate box. Figure 5. is an overlay of the co-polar pattern in the main cuts (phi = 0°, 45° ,90°, 135°) with and without the climate box. It is evident that within the conical range theta [-120°,120°], the pattern variation due to the presence of the climate box is negligible.

This test, de facto, shows that the climate box is practically RF transparent and therefore it does not affect either the impedance or the pattern shape of the AUT.
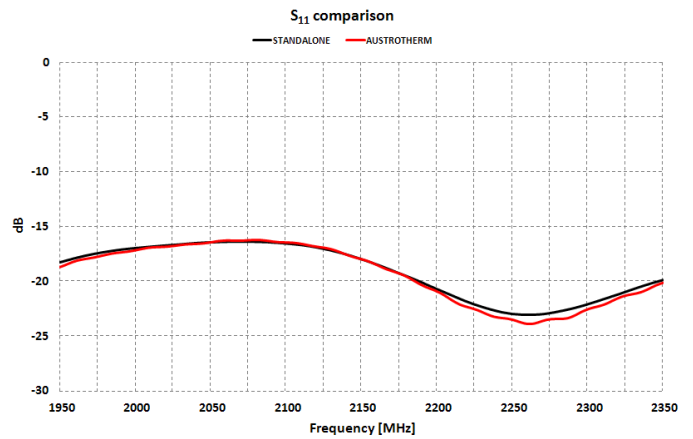
Figure 4.   Antenna return loss measured at room temperature with and without the climate box.
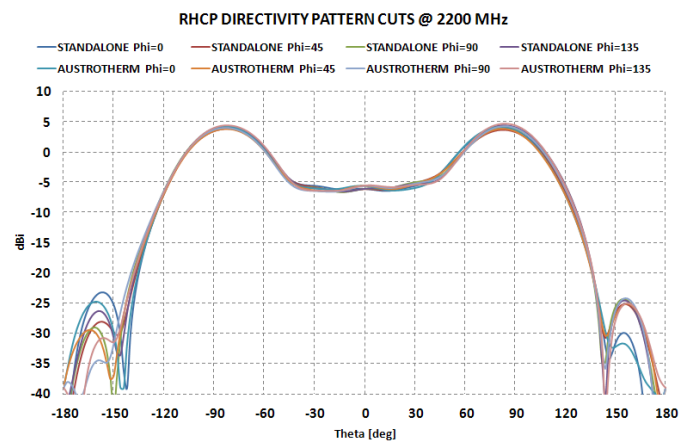
Figure 5.   Directivity pattern cuts @ 2.2GHz in circular polarisation at room temperature, with and without the climate box.

With this measurement setup we are able to evaluate directly the effect of the temperature variation on the antenna performance in terms of return loss and pattern.

IV.   PRELIMINARY THERMAL MEASUREMENT RESULTS

Before the beginning of the thermal cycle and in order to prevent the build-up of condensation over the AUT, a dry air flow has been injected throughout the container from the bottom holes to the upper ones at the top of the climate box, in order to evacuate the humid air inside the box. Figure 6 shows the temperature variation on the AUT surface over a half an hour thermal cycle, starting at room temperature and reaching almost -140°C, with a rate of approximately -5°C/min.

The AUT plus the climate box has overall dimensions within 220mm (diameter) and 400mm (height). Figure 8. shows the measurement setup in the MVG StarLab spherical near field measurement facility.

For such an AUT volume, a full 3D measurement can be performed at 9 frequencies, using an oversampling factor of x2 [8] in less than two minutes.
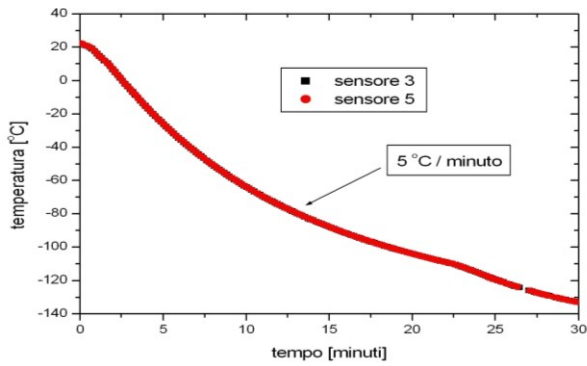
Figure 6.   Temperature changing curve as measured by thermistors 3 and 5 located at different positions on the antenna.
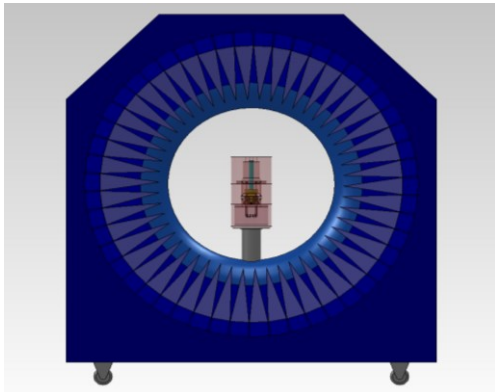
Figure 7.   Climate box enclosing the AUT and placed in the StarLab 18GHz Spherical NF measurement facility.

Due to the outstanding testing speed of the multi-probe spherical near field system, the thermal cycle in Figure 7 shows the possibility to measure the AUT at different desired frequencies in the same experiment, and ensure a negligible temperature variation during the single measurement.

V.   EXPERIMENTAL RESULTS

A quadrifilar helix antenna has been used as reference for the pattern and impedance measurement. The antenna operates in RHCP with a circularly symmetric radiation pattern. The RHCP and LHCP reference patterns at room temperature and without the thermal enclosure have been derived as an average over phi cuts and are shown in Figure 8.
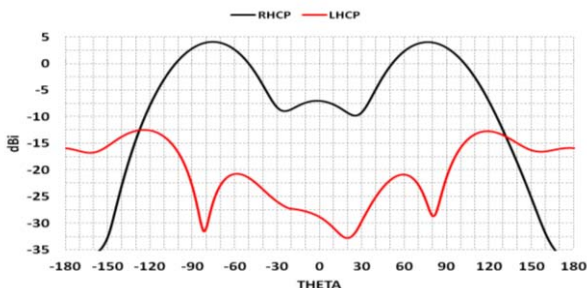
Figure 8.   Directivity patterns @2025MHz measured at room temperature in anechoic chamber.

During the thermal setup predisposition, three RFD thermistors have been attached to the antenna ground plane as shown in Figure 9 in order to monitor the temperature of the AUT during the thermal experiment.

Figure 9.   Detail of the AUT. RFD thermistors have been placed around the AUT ground plane.

The thermal measurement setup has been described in detail in Section III and the pertinent setup is shown in Figure 10. The measurement campaign test plan is hereafter reported:

- S11 measurement at room temperature including all surrounding environment;
- measurement repeatability evaluation, 3 successive radiation pattern measurements at room temperature;
- thermal radiation pattern testing at several temperature values, from room (+23°C) to cold (-105°C) conditions;
- S11 at cold temperature (-105°C) including all surrounding environment;
- visual inspection of the climate box (inner & outer) to check condensation build-up;
- S11 and pattern testing at room temperature including all surrounding environment.
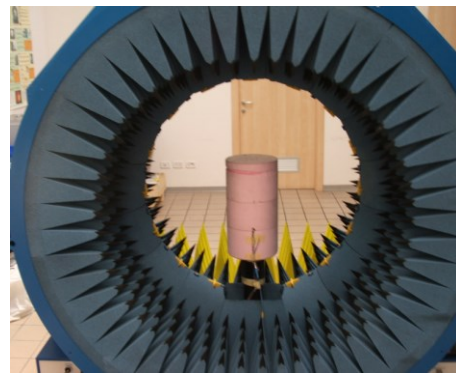
Figure 10.   Thermal measurement setup. The AUT is placed inside the climate box in the StarLab 18GHz Spherical Near Field measurement facility.

The test sequence is presented in the following, showing and discussing the obtained results. Before starting the thermal experiment, three measurements have been performed in order to evaluate the measurement repeatability. The first

measurement has been taken as reference and differential plots have been derived for the other two measurements.

Figure 11 and Figure 12 show that the repeatability performance of the measurements is very high particularly in correspondence with the RHCP peak directivity (theta = 70-75°), while it shows 0.1dB deviations on directivity values at 10dB below the peak. The LHCP repeatability results shows that a 1.4dB deviation is obtained in correspondence with values 35dB below peak (theta = 80°), while it remains below 0.5dB for lower value theta angles.
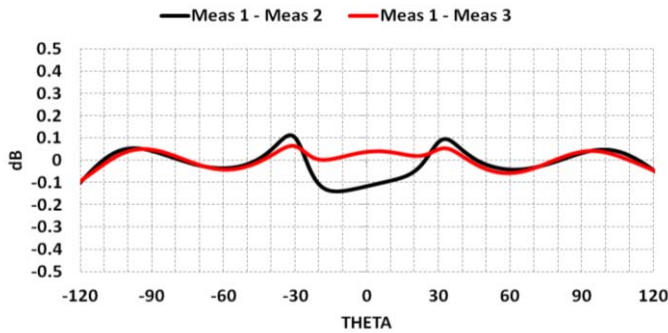
Figure 11.   RHCP patterns repeatability @ 2025MHz measured at room temperature, taking into account all the thermal measurement setup.
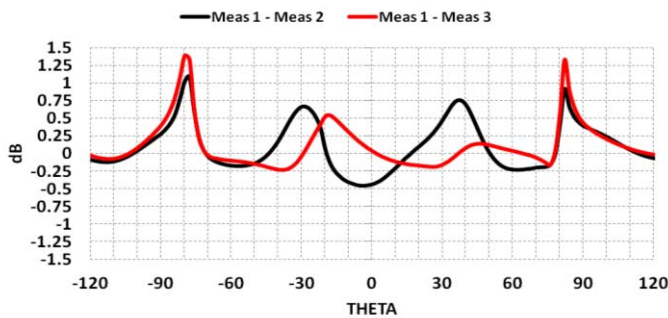
Figure 12.   LHCP patterns repeatibility @ 2025MHz measured at room temperature, taking into account all the thermal measurement setup.

Once the setup has been characterized, the liquid nitrogen has been poured into the bottom part of the climate box, as shown in Figure 13.

As described in detail in Section III, the AUT cooling has been achieved through heat conduction by means of an immersion chiller and a continuous dry air flow across the whole climate box. The temperature ramp applied to the AUT has been recorded with the data logger and it is displayed in Figure 14.

Several radiation pattern measurements have been performed during the thermal cycle shown in Figure 14. Upon reaching the lower bound temperature of -105°C for this experiment the final radiation pattern measurement has been carried out at this temperature before removing the liquid nitrogen.

Figure 13.   Pouring of the nitrogen in the climate box. The heat transfer is primarily provided by the immersion chiller shown.
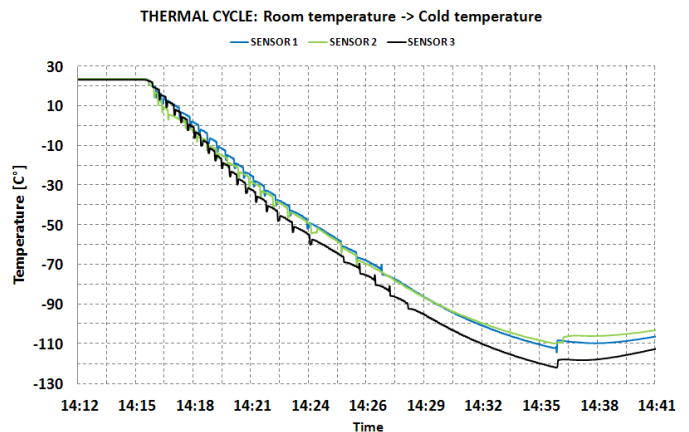
Figure 14.   Thermal cycle, from room (+23°C) to cold (-105°C) temperature.

The results presented are shown as a comparative measurement in order to isolate and investigate only the effect of temperature variation, minimizing any other variation contributions. The measurement performed just after pouring the liquid nitrogen into the bottom part of the climate box has been taken as reference for the comparative analysis. The reason is that liquid nitrogen with a dielectric constant around 1.45 [10] and the measurement setup including the climate box, PVC mast etc. have a minimum but measurable impact on the return loss and radiation pattern shape as discussed in Section IV.

The resulting comparative measurements are shown in Figure 15 for RHCP pattern and in Figure 16 for LHCP pattern. Figure 15 clearly shows that the temperature impact on the AUT co-polar pattern is minimal with a maximum 0.2dB deviation on directivity values up to 10dB below peak in the temperature range 20°C to -40°C /-60°C.The effect of the temperature is more evident at lower temperature levels around -105°C, where a maximum difference of 0.4dB is observed at theta = 30° on the co-polar pattern with directivity levels of -10dB below peak. The impact of the temperature on the cross-polar pattern is depicted in Figure 16. It is clear that the difference w.r.t the reference LHCP pattern is more evident, due to the fact that the plot is referred to directivity values 30dB below peak.
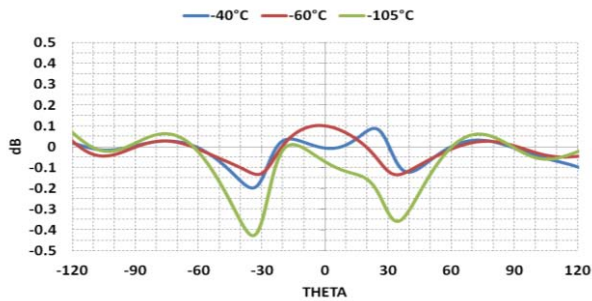
Figure 15.   Co-polar directivity differential results wrt room temperature.
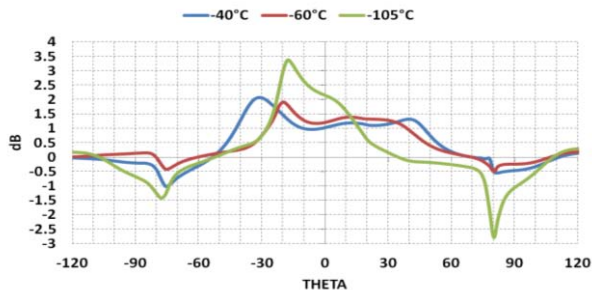
Figure 16.   Cross-polar directivity differential results wrt room temperature.

Once the temperature lower bound has been reached, liquid nitrogen has been removed from the bottom part of the climate box. A visual inspection of condensation build-up has been done by opening the container, highlighting the complete absence of condensation inside the climate box.

Several thermal radiation pattern measurements have been also performed during the temperature ramp from cold conditions to room temperature. Results obtained are equivalent to those obtained during the ramp from standard to cold conditions and for this reason are not shown. As denoted in the test plan, S_{11} measurements have been performed as well during the thermal cycle. In particular, Figure 17 shows the measured S_{11} at room temperature and at -105°C.

Some difference is visible at the low end of the band around 2025MHz, where the matching is approximately -25dB, while in the remaining part of the band the effect of temperature variation is negligible. It is important to note that the return loss measurement at -105°C might have been affected by minor uncertainties, due to the fact that the test cable has been moved during the thermal measurements.

VI.   CONCLUSIONS

In this paper the setup for thermal testing of an antenna in a near field spherical multiprobe system has been described. The method has been illustrated in this paper for the cold measurement with temperatures below -100°C but the extension to the full cold-hot temperature range is trivial. The bottom part has been filled with liquid nitrogen and the heat conduction mechanism has been designed in order to cool the AUT without the condensation build up on the AUT surface.
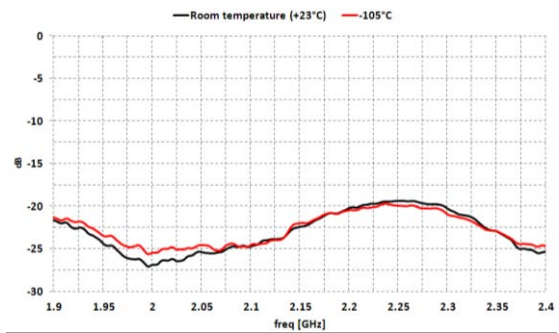
Figure 17. S_{11} acquired at room temperature and -105°C.

The thermal insulation is ensured by the climate box designed. The temperature is monitored thanks to the thermistors and the datalogger.

It has been demonstrated that the equipment designed leads to an excellent cooling of the AUT, ensuring at the same time a very good RF transparency and no major impact on the measurement equipment's temperature. Hence, the measurement of the AUT performances by means of the StarLab measurement facility could be easily performed without affecting the accuracy of the results.

The fast testing provided by the multiprobe system allows to measure the temperature dependence of an antenna at several different temperatures and frequencies within the same experiment, leading to a very efficient and cost effective thermal test campaign.

REFERENCES

[1]   The Institute of Electrical and Electronics Engineers, Inc, IEEE Standard Test Procedures for Antennas, IEEE Std. 149-1979;

[2]   J. Migl, J. Habersack, H. Grim, S. Paus, "Test Philosophy and Test Results of the Intelsat-IX C-Band Antennas", 25. AMTA 2003, Irvine, CA, US; 19.–24.10.2003;

[3]   L. J. Foged, A. Giacomini, R. Morbidini, " Thermal Testing of Antennas in Spherical Near Field Multi-Probe System", 5th European Conference on Antennas and Propagation, EuCAP 2011, Rome, Italy, April 2011;

[4]   J. E. Hansen (ed.), Spherical Near-Field Antenna Measurements, Peter Peregrinus Ltd., on behalf of IEE, London, United Kingdom, 1988;

[5]   P.O. Iversen, Ph. Garreau, K. Englund, E. Pasalic, O. Edvardsson, G. Engblom, "Real Time Spherical Near Field Antenna Test Range for Wireless Applications", Proc. Antenna Meas. Tech. Assoc., pp. 363 – 368, October 1999;

[6]   L. Duchesne, Ph. Garreau, N. Robic, A. Gandois, P.O. Iversen, G. Barone, "Compact multiprobe antenna test station for rapid testing of antennas and wireless terminals", 4th Mediterranean Microwave Symposium, Marseille 2004;

[7]   Ph. Garreau, L. Duchesne, A. Gandois, L. Foged, P. Iversen "Probe array concepts for fast testing of large radiating structures", Proc. Antenna Meas. Tech. Assoc., pp. 159-164, October 2004;

[8]   L.J. Foged, A. Scannavini, "Efficient testing of wireless devices from 800MHz to 18GHz, Radio Engineering Magazine, Vol 18, No 4, December 2009;

[9]   http://www.satimo.com/content/products/starlab;

[10]   NASA Tech Briefs, Jun 2001by Roth, Tim E, "Capacitive sensor for measuring level of liquid nitrogen";

[11]   Austrotherm   XPS   -   extruded   polystyrene   foam, http://en.austrotherm.com/front_content.php?idart=197;

[12]   Huber+Suhner RF coaxial cable, http://www.hubersuhner.com